ELSEVIER

Thin Solid Films 417 (2002) 67–71

thin solid films

www.elsevier.com/locate/tsf

Orientation dependence of magneto-resistance behaviour in a carbon nanotube rope

G.C. McIntosh[a], G.T. Kim[b,c], J.G. Park[a], V. Krstic[b], M. Burghard[b], S.H. Jhang[a], S.W. Lee[a], S. Roth[b], Y.W. Park[a,*]

[a]*Department of Physics, Seoul National University, Seoul 151-742, South Korea*
[b]*Max Planck Institut fuer Festkoerperforschung, Heisenbergstrasse 1, D-70569 Stuttgart, Germany*
[c]*Department of Electrical Engineering, Korea University, Seoul 136-701, South Korea*

Received 1 May 2002; accepted 13 June 2002

Abstract

The orientation dependence of magneto-resistance behaviour for a single-walled carbon nanotube (SWCN) rope is reported. A clear delineation of behaviours is observed between applying a magnetic field perpendicular or parallel to the rope axis. For a perpendicular field, monotonic negative magneto-resistance is observed due to two-dimensional weak localisation within the rope. By contrast, for a parallel field, complicated oscillatory behaviour is observed due to the Altshuler–Aronov–Spivak effect around closed electron trajectories on discrete cylinders within the SWCN rope. A dominant oscillatory mode can be identified which corresponds to closed paths around the outer circumference of the SWCN rope. However, due to the composite filamentary nature of the rope, the overall oscillatory behaviour is rather complicated and can be classified as universal conductance fluctuations. With a backgate voltage applied to the sample, Coulomb blockade peaks are observed in the transport current with additional peak structure superimposed due to resonant tunnelling. We find an interesting effect whereby these peaks are suppressed in the presence of a magnetic field.

Keywords: Carbon nanotubes; Magneto-resistance

1. Introduction

Carbon nanotubes [1–3] are of considerable interest due to the fundamental physics aspects which they allow to be explored [4]. Due to their mesoscopic dimensions, interesting quantum interference effects are expected to occur. For example, with a cylindrical structure, carbon nanotubes are ideal for observing the Altshuler–Aronov–Spivak effect when a magnetic field is applied along their axis. This has been reported for an individual multi-walled carbon nanotube (MWCN) whereby oscillations are seen in the measured magneto-resistance [5] and agreement with theory is excellent. Here, the concentric nanotube cylinders comprising a MWCN are effectively decoupled with only one cylinder likely metallic. Hence, from an electronic transport point of view, the MWCN effectively behaves as a single-walled carbon nanotube (SWCN), albeit with a large diameter [5]. The quantum mechanical nature of a carbon nanotube is also manifest along the longitudinal direction where, in metallic carbon nanotubes, phase coherence of the charge carrier wavefunction can be maintained for distances up to several micrometers, even in the presence of defects [6]. This demonstrates the robust, mesoscopic nature of carbon nanotubes.

Another manifestation of quantum interference effects is the observation of weak localisation in magneto-resistance experiments. Here, phase coherence is maintained in closed electron trajectories interior to the carbon nanotube system which becomes disrupted in the presence of a magnetic field. Magneto-resistance measurements have been carried out on carbon nanotube bundles [7,8], mats [9], thin films [10], and also individual MWCNs [11–13]. For low temperatures and low

*Corresponding author. Tel.: +82-2-880-6607; fax: +82-2-873-7037.
E-mail address: ywpark@phya.snu.ac.kr (Y.W. Park).

0040-6090/02/$ - see front matter © 2002 Elsevier Science B.V. All rights reserved.
PII: S0040-6090(02)00592-8

magnetic fields, negative magneto-resistance behaviour is typically observed which can be attributed to two-dimensional weak localisation. Apart from the case of a MWCN, magneto-resistance measurements have typically only been carried out with a magnetic field applied transverse to the carbon nanotube system. As demonstrated in this paper, it is also worthwhile to carry out the measurements with a field applied parallel to the carbon nanotube system. For a carbon nanotube rope, due to the specific geometric configuration in the parallel direction and multi-filamentary nature, interesting behaviour apart from simple negative magneto-resistance can be expected to occur. In particular, we have carried out magneto-resistance measurements on a SWCN rope with a magnetic field applied both perpendicular and parallel to the rope axis and we observe markedly different behaviour between the two cases. The results of these measurements are presented below.

2. Sample preparation

The method followed for synthesizing and preparing our SWCN rope sample is well established [14,15]. SWCNs were produced using an arc discharge furnace with Ni/Y as the catalyst. Measurements with transmission electron microscopy reveal the individual SWCNs produced by this method to have a typical diameter of $\simeq 1.5$ nm. This is important since it is expected that SWCNs produced with this vicinity of diameter will be of the metallic (10,10) armchair variety [16]. Such a situation is required so that our sample involves a metallic SWCN rope. Purification of the SWCNs was carried out using a centrifuge.

A Si wafer with a 300-nm thick thermally grown oxide layer was used as a substrate. A SWCN rope was first deposited onto the substrate and then electrodes were fabricated over the SWCN rope. The motivation for using this configuration is to achieve a low contact resistance between the SWCN rope and electrodes. To promote adsorption of the SWCNs onto the substrate, the wafer was first treated with 3-(aminopropyl) triethoxysilane.

A 4-probe electrode was then produced by covering the substrate with a two-layer poly(methyl methacrylate) resist system and electron beam lithography was used to define the electrodes. Afterwards, cobalt was evaporated onto the substrate. The use of cobalt for the electrode metal is of interest because, being a ferromagnetic metal, this may facilitate the observation of spin-orientated transport through our carbon nanotube rope [17]. The final lift-off process was performed during which the undesired metal was removed by mechanical stress. Using this method, the resulting sample is shown in Fig. 1. A long horizontally aligned SWCN rope can be seen through the central region of Fig. 1. This

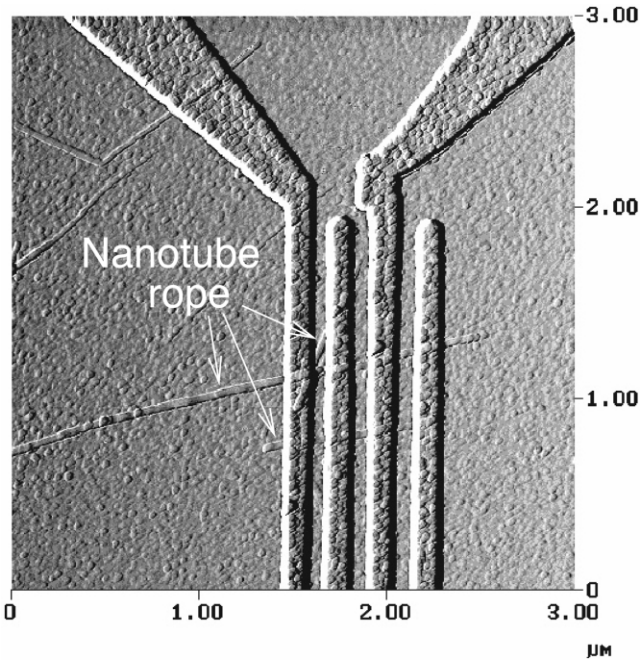

Fig. 1. SFM image of a Co 4-probe electrode deposited over SWCN ropes.

appears as a 'clean' and straight structure, without obvious imperfections such as catalyst impurities.

All electronic transport measurements were carried out between the left two electrodes of our sample, where the contact resistance was found to be $\sim 100\ \mathrm{k}\Omega$. This is sufficiently low so that our magneto-resistance measurements will not be overly complicated by Coulomb blockade phenomena. The magneto-resistance of our sample was measured for both perpendicular and parallel magnetic field orientations; whereby the parallel field direction is along the axis of the long horizontal SWCN rope in Fig. 1 and the perpendicular field is applied perpendicular to the substrate.

In addition to the long SWCN rope, two shorter SWCN ropes can be seen beneath the electrodes in the same vicinity; one aligned horizontally with the long SWCN rope and the other aligned vertically away from the long SWCN rope. For parallel and perpendicular applied magnetic fields, the vertically aligned SWCN rope is perpendicular to the applied magnetic field in both cases. Hence, this SWCN rope is not considered as significant in contributing to the main differences we observe between the perpendicular (Fig. 2a) and parallel (Fig. 2b) magnetic field cases. Regarding the short horizontally aligned SWCN rope, we were unable to detect oscillatory modes in our magneto-resistance data which might correspond to quantum interference between this and the long horizontally aligned SWCN rope. Hence, in the following, we can attribute the main difference in measured magneto-resistance behaviour between the perpendicular and parallel magnetic field

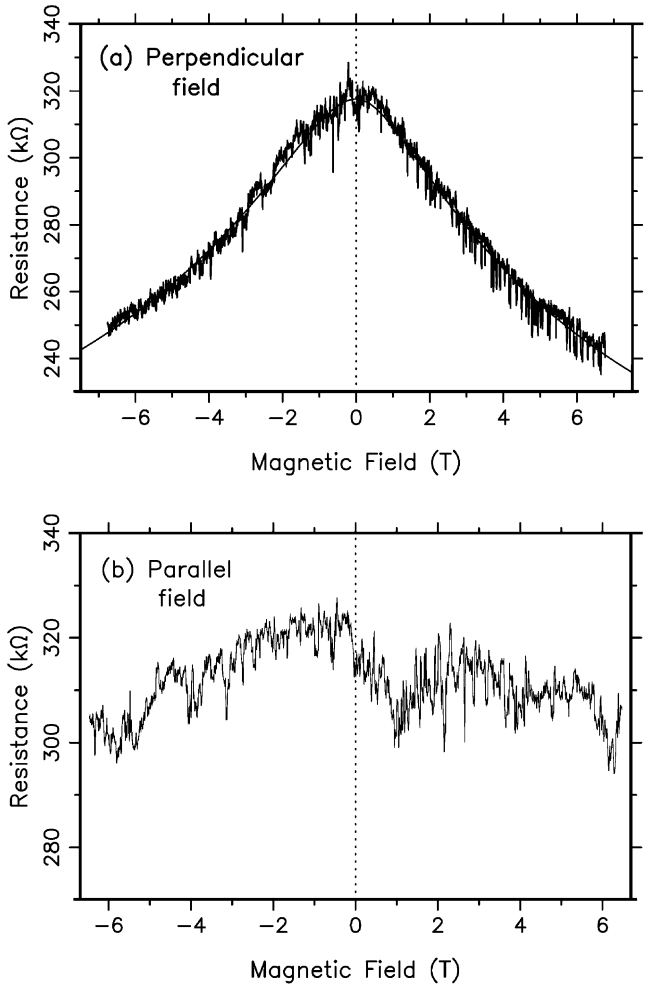

Fig. 2. Magneto-resistance for a field applied (a) parallel and (b) perpendicular to the SWCN rope axis. The solid curve in (a) is a fit to two-dimensional weak localisation, Eq. (1).

cases as arising from either of the two horizontally aligned SWCN ropes in Fig. 1.

3. Perpendicular magneto-resistance behaviour

The magneto-resistance measured for our sample is shown in Fig. 2. These measurements were carried out at a temperature of 4.2 K for a magnetic field applied perpendicular (Fig. 2a) and parallel (Fig. 2b) to the long SWCN rope axis (and to the substrate). In Fig. 2a, we see monotonic negative magneto-resistance behaviour similar to that seen by previous workers [7–11]. This behaviour is generally attributed to weak localisation, often two-dimensional. We confirm this for our case as follows.

Two-dimensional weak localisation is theoretically predicted to have the following form [18],

$$\Delta\sigma_{2D} = \frac{e^2}{2\pi^2\hbar}\left(\psi\left(\frac{1}{2}+\frac{1}{x}\right)+\ln(x)\right), \qquad (1)$$

where $x = L_{Th}^2 4eB/\hbar$. Here, e is the electron charge, $2\pi\hbar$ is Planck's constant, ψ is the digamma function, B is the applied magnetic field and L_{Th} is the decoherence length. Fits of Eq. (1) to our data are given by the solid curve in Fig. 2a. From this fit, we obtain a dephasing length of $L_{Th} = 14.1$ nm for $B < 0$ and $L_{Th} = 14.7$ nm for $B > 0$. Considering that, from Fig. 1, we can estimate a diameter for the nanotube rope of ~ 30 nm, these values seem quite reasonable. Since weak localisation is expected to occur in a disordered metal, in our case the disorder would arise within the rope due to its composite multi-filamentary nature.

An expression for one-dimensional weak localisation can also be fit to the data in Fig. 2a. However, the dephasing lengths obtained are virtually identical to the two-dimensional case. These values are less than the diameter of our carbon nanotube rope, implying that one-dimensional weak localisation is not valid for this case. We also find a problem when attempting to relate three-dimensional weak localisation to the data in Fig. 2a. Three-dimensional weak localisation is expected to have a B^2-dependence at low fields and a $\sqrt{B}$-dependence at high fields. While a B^2-dependence could very well apply to our data at low fields, for higher fields the data decreases faster than the $\sqrt{B}$-dependence. Hence, we also dismiss the three-dimensional case. In summary, we conclude that the negative magneto-resistance behaviour seen in Fig. 2a is due to two-dimensional weak localisation.

4. Parallel magneto-resistance behaviour

For a magnetic field applied parallel to the long SWCN rope axis in Fig. 1, the measured magneto-resistance is given in Fig. 2b. These data also seem to show a very weak component of negative magneto-resistance behaviour which could arise from the short vertically aligned SWCN rope in Fig. 1. However, apart from this, the behaviour is considerably different from the perpendicular case of Fig. 2a. Despite the appearance of noise in the data of Fig. 2b, we can consider the possibility that complicated oscillatory behaviour is also present. To pursue this possibility we have carried out a Fourier transform of the data for fields $B > 0$, shown in Fig. 3. We find that a multitude of modes are indeed present, but mostly the frequency structure is rather complicated and it is difficult to identify dominant modes. The only exception is a dominant mode appearing at $1/B = 0.4\ T^{-1}$. By contrast, a Fourier transform of the data in Fig. 2a reveals no significant frequency modes apart from that due to the clearly visible functional dependence fit by Eq. (1). This indicates that the rapidly varying behaviour in Fig. 2a is indeed pure random noise.

For a magnetic field parallel to a cylindrical structure such as a SWCN, oscillations are expected to occur in

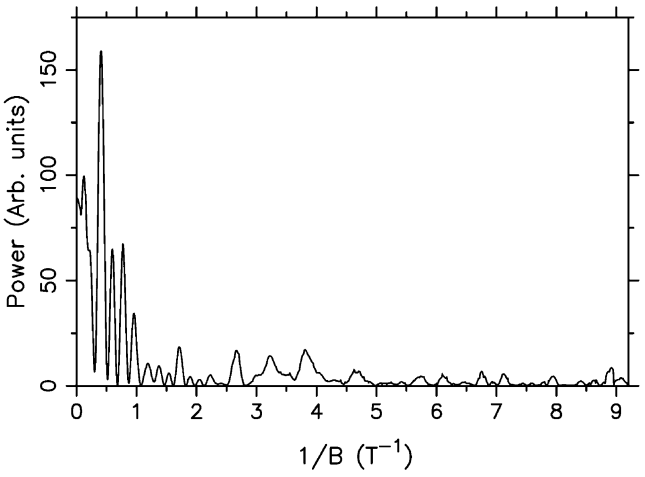

Fig. 3. Power spectrum for the Fourier transform of the magneto-resistance data in Fig. 2b for fields $B>0$ T.

the magneto-resistance due to the Altshuler–Aronov–Spivak effect [5]. The period for these oscillations is given by $\Delta B=h/2e\pi r^2$ where r is the cylinder radius. Such oscillations have been observed in MWCNs where agreement between theory and experiment is excellent [5]. The dominant mode appearing at $1/B=0.4$ T^{-1} in Fig. 3 corresponds to a cylinder radius of $r=16$ nm. Given that, from Fig. 1 we can estimate a diameter for the SWCN ropes of $\sim$30 nm, this gives good agreement for closed electron trajectories to occur around the outer circumference of the nanotube rope.

Given the multi-filamentary nature of our nanotube rope, the remaining complicated oscillatory structure in Fig. 2b would arise from the multitude of closed trajectories available within the rope and the interference amongst these trajectories. In this regard, the complicated structure seen in Fig. 2b could be classified as universal conductance fluctuations (UCFs). Such behaviour is expected to occur in a mesoscopic system such as our sample [19]. Furthermore, the amplitude of the fluctuations in Fig. 2b is the order of $h/e^2=25.8$ kΩ which is expected for UCFs. We should emphasize that the pattern associated with UCFs is not purely random noise in the statistical sense but is reproducible. Repeating the measurement without varying the measurement conditions, such as temperature or impurity configuration, would yield exactly the same pattern. The presence of UCFs indicates that the electron wavefunctions for the various trajectories have not been significantly dephased along the sample length. Hence, we could use this information to estimate a coherence length of at least $\sim$100 nm (the electrode spacing in Fig. 1) along the length of the nanotube rope.

5. Coulomb blockade behaviour

As well as measuring magneto-resistance behaviour, we have also attached a backgate electrode to our sample and measured the variation of transport current with varying gate voltage. The result of this is given in Fig. 4. Despite the relatively low contact resistance of our sample, peak structure is evident in Fig. 4, indicating that Coulomb blockade phenomena is present. However, the peak amplitude is quite weak and tending towards the average current value which would apply if the Coulomb blockade phenomena was absent. In the absence of a magnetic field, we observe two large peaks with finer structure superimposed. For example, for $V_G<0$ we find six smaller sub-peaks sitting on top of a single large peak.

From our previous investigations of Coulomb blockade phenomena [20] we can understand this peak structure as follows. The two large peaks are due to pure Coulomb blockade phenomena. The sub-peaks originate from resonant tunnelling through discrete energy levels of our sample whereby, due to the mesoscopic dimensions involved, energy levels become discretized. In particular, with a finite length along the longitudinal direction, our sample can be considered in terms of a one-dimensional square well [21]. For example, from Fig. 1, we could estimate that the long SWCN rope has a length of at least 3 μm. For the corresponding one-dimensional square well, this gives an energy level spacing of $\Delta E\sim0.6$ meV. This can be related to the sub-peak spacing in Fig. 4 for $B=0$ using $\Delta V_G=\Delta E/e\alpha$ where α is a measure of the coupling between the gate electrode and sample. That is, $\alpha=C_G/C$ where C_G is the capacitance between the gate and the SWCN rope sample while C the total capacitance between the sample and its environment. From Fig. 4, we estimate an average spacing for the sub-peaks of $\Delta V_G=0.77$ V. This yields $\alpha=0.00078$. This tiny value for α highlights the poor coupling between the gate electrode and sample. Using $\Delta V_G=(U+\Delta E)/e\alpha$, where ΔV_G is the spac-

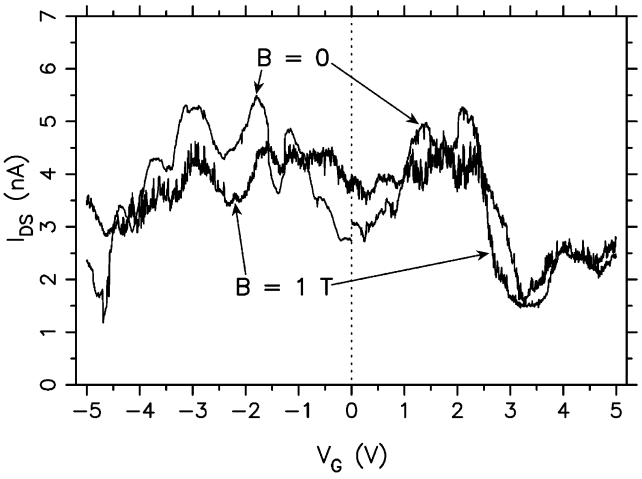

Fig. 4. Transport current with a substrate backgate voltage applied; in the presence and absence of a magnetic field.

ing for major Coulomb blockade peaks [22], we can also estimate the charging energy, U, of our sample due to Coulomb blockade phenomena. We estimate $U \simeq 3.0$ meV. Our ratio of U to ΔE is in agreement with other workers [21,22]. This information also indicates that ballistic transport is occurring through our sample over a length of at least 3 μm. This further highlights the robust mesoscopic nature of our SWCN sample.

In Fig. 4 we also demonstrate the effect on this peak structure when a magnetic field of 1 T is applied. Interestingly, the peak structure becomes suppressed in a similar fashion, regardless of whether the field is applied perpendicular or parallel to the rope axis. Since the effect is virtually identical for a parallel or perpendicular configuration, this rules out effects such as weak localisation or the Ahranhov–Bohm effect since these effects depend heavily on the geometry of the situation. These geometries are vastly different between the parallel and perpendicular cases. Instead, the effect must only depend on a scalar quantity such as energy.

One obvious means by which the charge carrier's energy can be affected in the presence of a magnetic field is through Zeeman splitting. For a field of 1 T, the Zeeman energy for an electron is $\simeq 0.12$ meV. This is a significant fraction of the discrete energy level spacing, $\Delta E \simeq 0.6$ meV, estimated above. Hence, in the presence of a magnetic field the peak structure in Fig. 4 would be shifted by this factor. This shift will occur up or down depending on the orientation of the transported spins with respect to the applied magnetic field. The multi-component nature of our sample could allow two spin configurations to be transported in parallel. With the peak structure from each contribution shifting in opposite directions, they become merged and averaged out. This may provide an explanation for the behaviour seen in Fig. 4.

The fact that the transport current through our SWCN rope has a dependence on an applied magnetic field implies that the charge carrier's spin plays a role in the transport. Hence, we have the possibility of a spin-electronic device using our SWCN rope [17].

Acknowledgments

This work was supported by the Ministry of Information and Communication (MIC), Korea. Partial support for GCM was provided by the BK21 project of the Ministry of Education (MOE), Korea.

References

[1] S. Iijima, Nature 354 (1991) 56.
[2] J.W. Mintmire, B.I. Dunlap, C.T. White, Phys. Rev. Lett. 68 (1992) 631.
[3] N. Hamada, S. Sawada, A. Oshiyama, Phys. Rev. Lett. 68 (1992) 1579.
[4] C. Dekker, Phys. Today 52 (1999) 22.
[5] A. Bachtold, C. Strunk, J.-P. Salvetat, J.-M. Bonard, L. Forró, T. Nussbaumer, C. Schönenberger, Nature 397 (1999) 673.
[6] P.L. McEuen, M. Bockrath, D.H. Cobden, Y.-G. Yoon, S.G. Louie, Phys. Rev. Lett. 83 (1999) 5098.
[7] S.N. Song, X.K. Wang, R.P.H. Chang, J.B. Ketterson, Phys. Rev. Lett. 72 (1994) 697.
[8] M. Baxendale, V.Z. Mordkovich, S. Yoshimura, R.P.H. Chang, Phys. Rev. B 56 (1997) 2161.
[9] G.T. Kim, E.S. Choi, D.C. Kim, D.S. Suh, Y.W. Park, K. Liu, G. Duesberg, S. Roth, Phys. Rev. B 58 (1998) 16064.
[10] G. Baumgartner, M. Carrard, L. Zuppiroli, W. Basca, W.A. de Heer, L. Forró, Phys. Rev. B 55 (1997) 6704.
[11] L. Langer, V. Bayot, E. Grivei, J.-P. Issi, J.P. Heremans, C.H. Olk, L. Stockman, C. Van Haesendonck, Y. Bruynseraede, Phys. Rev. Lett. 76 (1996) 479.
[12] J.-O. Lee, J.-R. Kim, J.-J. Kim, J.-H. Kim, N. Kim, J.-W. Park, K.-H. Yoo, K.-H. Park, Phys. Rev. B 61 (2000) 16362.
[13] A. Fujiwara, K. Tomiyama, H. Suematsu, M. Yumara, K. Uchida, Phys. Rev. B 60 (1999) 13492.
[14] C. Journet, P. Bernier, Appl. Phys. A 67 (1998) 1.
[15] C. Journet, W.K. Maser, P. Bernier, A. Loiseau, M.L. Delachapelle, S. Lefrant, P. Deniard, R. Lee, J.E. Fischer, Nature 388 (1997) 756.
[16] A. Thess, R. Lee, P. Nikolaev, H. Dai, P. Petit, J. Robert, C. Xu, Y.H. Lee, S.G. Kim, D.T. Colbert, G. Scuseria, D. Tománek, J.E. Fischer, R.E. Smalley, Science 273 (1996) 483.
[17] K. Tsukagoshi, B.W. Alphenaar, H. Ago, Nature 401 (1999) 572.
[18] P.A. Lee, T.V. Ramakrishnan, Rev. Mod. Phys. 57 (1985) 287.
[19] P.A. Lee, A. Douglas Stone, H. Fukuyama, Phys. Rev. B 35 (1987) 1039.
[20] G.C. McIntosh, G.T. Kim, J.G. Park, V. Krstic, S. Roth, Y.W. Park, Curr. Appl. Phys. 1 (2001) 321.
[21] S.J. Tans, M.H. Devoret, H. Dai, A. Thess, R.E. Smalley, L.J. Geerligs, C. Dekker, Nature 386 (1997) 474.
[22] M. Bockrath, D.H. Cobden, P.L. McEuen, N.G. Chopra, A. Zettl, A. Thess, R.E. Smalley, Science 275 (1997) 1922.